Journal of Applied Polymer Science

Influence of Thermooxidative Aging on the Static and Dynamic Mechanical Properties of Long-Glass-Fiber-Reinforced Polyamide 6 Composites

Xiaoling Zuo, Kaizhou Zhang, Yang Lei, Shuhao Qin, Zhi Hao, Jianbing Guo
National Engineering Research Center for Compounding and Modification of Polymeric Materials, College of Materials Science and Metallurgy, Guizhou University, Guiyang, Guizhou, China
Correspondence to: Z. Hao (E-mail: hz780104@sina.com) or J. Guo (E-mail: guojianbing_1015@126.com)

ABSTRACT: The static and dynamic mechanical properties, thermal behaviors, and morphology of pure long-glass-fiber-reinforced samples [polyamide 6 (PA6)/long glass fiber (LGF)] with different thermal exposure times at 160°C were studied by comparison with stabilized samples in this study. The aging mechanism of the PA6/LGF samples under heat and oxygen was studied with the methods of thermal Fourier transform infrared (FTIR), differential scanning calorimetry, dynamic mechanical analysis, scanning electron microscopy (SEM), and so on. The results indicate that the static mechanical strength, melting temperature, and crystallization temperature decreased because of the decomposition of the macromolecular chain of PA6 resin and the debonding of the interface between the glass fibers and matrix. The glass-transition temperature and crystallinity also increased and decreased, respectively, after aging. The macromolecular chain decomposition dominated in the subsequent aging process; this resulted in many sharp and brittle microcracks appearing on the surfaces of the aged samples, as shown by SEM and the FTIR spectra. The existence of stabilizers endowed the PA6/LGF composites with better retention of static and dynamic mechanical properties. The reason was that the metal ions of the copper salt antioxidant acted as an anti-aging catalyst in the reinforced PA6 system. © 2013 Wiley Periodicals, Inc. J. Appl. Polym. Sci. **2014**, *131*, 39594.

KEYWORDS: aging; differential scanning calorimetry (DSC); glass transition; polyamides; thermal properties

Received 31 December 2012; accepted 23 May 2013
DOI: 10.1002/app.39594

INTRODUCTION

In recent years, there has been strong growth in the use of long-glass-fiber-reinforced thermoplastic composites in semi-structural and engineering applications.[1–4] Glass-fiber-reinforced polyamides are excellent composite materials in terms of their high levels of mechanical performance and temperature resistance. In view of engineering applications, long-glass-fiber-reinforced polyamide composites have more broad prospects for development.[5,6] However, in the processes of machining, storage, and application, composites come in contact with air, water, sunshine, and other environment factors and are more sensitive and vulnerable to those factors.[7–9] Glass-fiber-reinforced polyamides are excellent composite materials, but the mechanical properties of polyamide-based composites decrease markedly because of the absorption of water and other polar fluids.[10–12] Therefore, aging studies of composites in natural environments is important.

Thermooxidative aging is the one of main aging forms of composite materials and is the result of the integrated effects of heat and oxygen. Heat accelerates polymer oxidation, whereas the decomposition of oxides leads to the auto-oxidation scission of the main chain.[13,14] It has been suggested that mechanochemical chain scission is the primary beginning process; this results in the formation of hydroperoxides, which is the cause of subsequent oxidation during the process of the polymer yielding macroalkyl radicals.[15,16] The oxidation of polyamides proceeds by a free-radical chain reaction and is accompanied by an autoretardant accumulation of peroxides and carbonyl groups.[17,18] Thermal and oxidative embrittlement behaviors influence each other and are usually applied in the analysis of the static and dynamic mechanical properties of aged polymers. Thermal embrittlement can promote oxidative embrittlement, which occurs primarily on the weak bonds of the molecular chain of the amorphous region.[19]

Polyamide 6 (PA6), prepared by the hydrolytic polycondensation of caprolactam monomer in the presence of a monofunctional acid, shows a higher ratio of carboxylic groups to amino end groups; this makes the polymer more sensitive to oxidation.[20,21] PA6 has a high heat distortion temperature and good

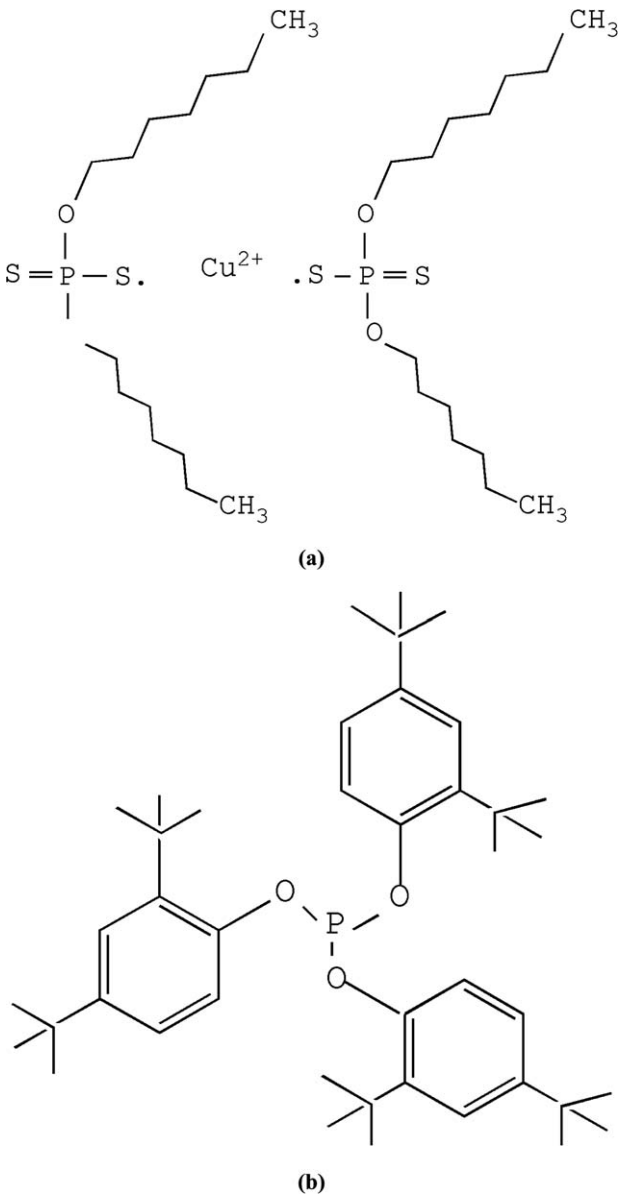

Figure 1. Structure of the (a) copper salt antioxidant and (b) phosphorous acid antioxidant 168.

mechanical properties, such as tensile strength and tensile modulus; long-glass-fiber-reinforced PA6 composite materials are able to be used in high-temperature environments. However, when this polymer is exposed to a high temperature for a prolonged period, the polymer generally starts to show discoloration and a decrease in its static and dynamic mechanical properties.[22] The macroscopic mechanical behaviors of long-aged composite materials at the interface/interphase between the matrix and the fiber can be investigated by dynamic mechanical analysis (DMA).[23] Chemical aging may be the result of thermal, oxidative, or hydrolytic reactions, and to prevent oxidation, certain types of stabilizers can be added to PA6, such as radical scavengers, hydroperoxide decomposers, copper salt antioxidants, hindered phenols, and phosphite antioxidants. The frequently used antioxidants are classified into two categories. The primary one is the so-called chain stoppers because they donate hydrogen atoms and stop the free-radical chain reaction of oxidation. These primary antioxidants include phenols and amines. The secondary antioxidants convert hydroperoxide to some more stable products, and then, autocatalytic degradation reactions are prevented.[24] For example, the efficiency of phenolic antioxidants has been ascribed to hydrogen bonding between amide groups in polyamides and the hydroxyl groups of the phenolic antioxidants and to the kinetic chain length shown by polyamides.[25,26]

In this study, dumbbell-shaped injected samples of PA6/long glass fiber (LGF) were used for the systematic study of thermooxidative aging behaviors; the samples were subjected to oven aging at different times under 160°C. The static and dynamic mechanical properties of the aged PA6/LGF composites were characterized by thermogravimetric analysis, differential scanning calorimetry (DSC), DMA, Fourier transform infrared (FTIR) spectroscopy,

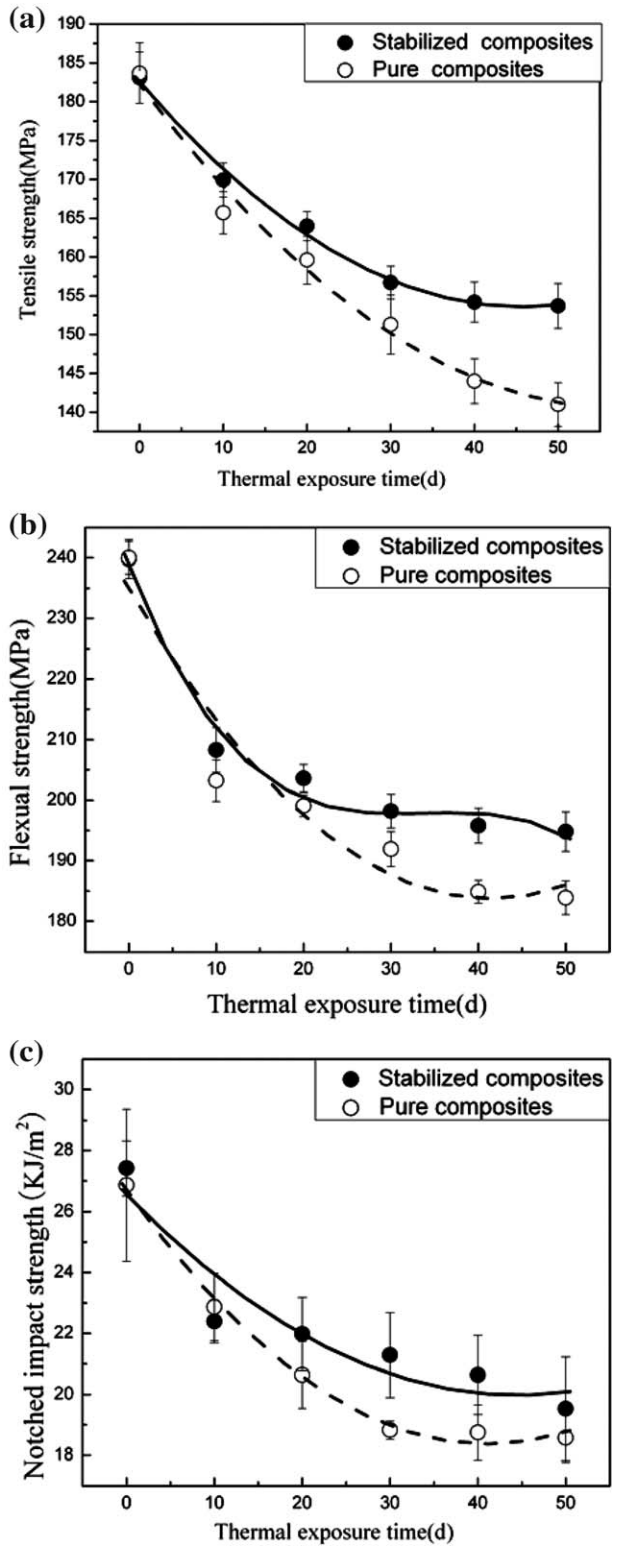

Figure 2. Effect of the thermal aging on the mechanical properties for two kinds of thermally exposed PA6/LGF samples: (a) tensile strength, (b) flexural strength, and (c) notched impact strength.

and scanning electron microscopy (SEM). The aging behaviors of the PA6/LGF samples stabilized with commonly used industry stabilizers in contrast with that of the pure samples.

EXPERIMENTAL

Materials

The PA6 resin we used was a low-viscosity-grade product produced by UBE Co., Ltd. (Japan, 1013B). The copper salt antioxidant [see Figure 1(a)] was produced by Brueggemann Co., Ltd. (Germany, H161). The phosphorous acid antioxidant 168 [see Figure 1(b)] was produced by Ciba Co. (Switzerland). The continuous glass fiber rovings were a commercial product made by Chongqing Polycompany International Corp. (China), with an average diameter of 17 μm, grade ECT4301H, and a linear density of 2400 tex.

Preparation of the Composites

The materials applied in this study were pure and stabilized PA6/LGF composites. The stabilized PA6/LGF composites were prepared by a synchronized antioxidant system of 0.3-phr addition of copper salt antioxidant and phosphorous acid antioxidant 168. PA6 was dried before used for 10 h at 80°C in an oven to remove any moisture. Both the pure and stabilized composites were blended in a twin-screw extruder (TSE-40A, length/diameter = 40, diameter = 40 mm, Coperion Keya Machinery, Co., Ltd., Nanjing, China) at 205–250°C, and the contents of the glass fibers were kept at constant at 30 wt %. An impregnation groove was used for the accommodation of polymer melting with a temperature control unit, which set the temperature of the groove at 290°C. The continuous strand was then chopped into pellets at a length of 12 mm for injection molding. The extrudates were dried at 80°C for 24 h. The resulting composites were then injection-molded (machine type CJ80M3V, Chen De Plastics Machinery Co., Ltd., Guangdong, China) at 235–290°C into various samples for testing and characterization. Both the pure and stabilized PA6/LGF samples were thermooxidized in an oven at 160°C for 0, 10, 20, 30, 40, and 50 days, respectively. The samples were taken out at a regular time intervals and subjected to performance testing and structural characterization. The temperature fluctuations in the oven were ±1°C.

Measurements

Static and Dynamic Mechanical Properties. The impact strengths were determined with an impact tester (ZBC-4B) according to GB/T1043-2008; the notch depth was 2 mm, and the angular radius of the notch was 0.2 mm. Tensile stress–strain and flexural tests were performed with a WDW-10 electronic universal tensile stress tester according to GB/T1040-2006 and GB/T9341-2008 standards, respectively.

The dynamic mechanical properties were studied with a Q800 Metravib RDS viscoanalyzer at a heating rate of 2°C/min over a temperature range from −30 to 150°C. The samples (60 × 10 × 4 mm^3) were tested with an imposed frequency of 10 Hz and an oscillation amplitude of 10 μm in the bending mode. The purpose of this analysis was the determination of the main relaxation characteristics at different aging times.

DSC. The thermal properties of the samples were studied on a DSC instrument (TA Instruments, Q-10, New Castle, DE) in a nitrogen atmosphere with a flow rate of 40 mL/min. Each of the samples of about 5 mg was loaded in an aluminum sample pan were heated from 40 to 260°C at 10°C/min.

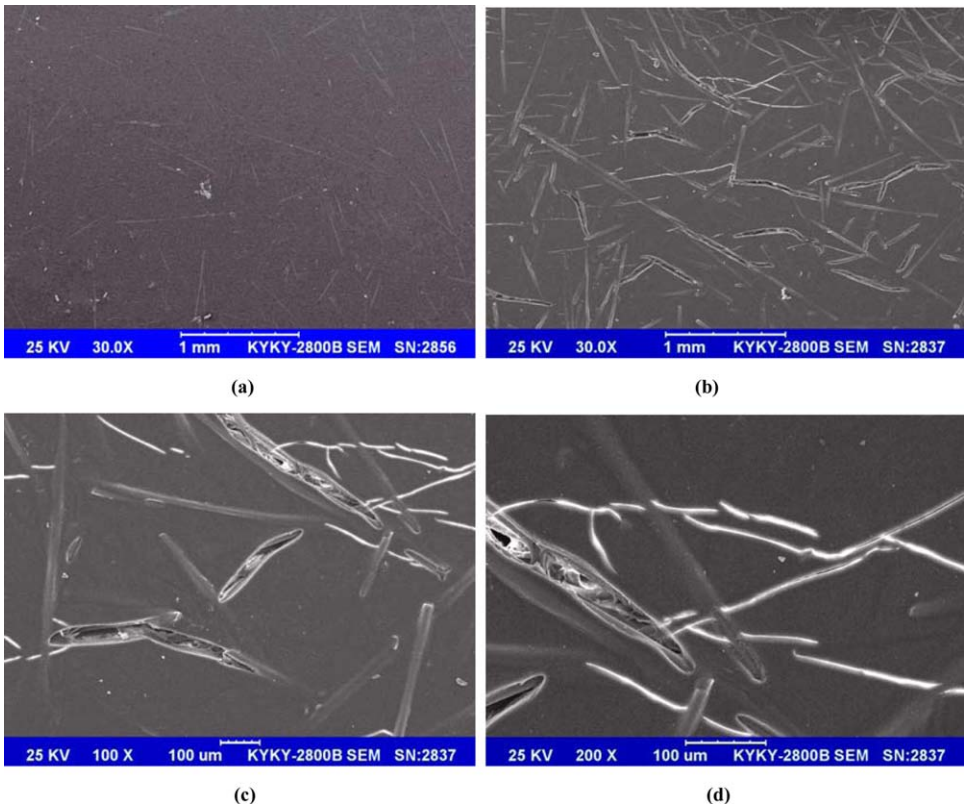

Figure 3. Scanning electronic micrographs of the surfaces of unaged sample and PA6/LGF sample aged for 50 days: (a) unaged sample with 30× magnification, (b) sample aged for 50 days with 30× magnification, (c) sample aged for 50 days with 100× magnification, and (d) sample aged for 50 days with 200× magnification. [Color figure can be viewed in the online issue, which is available at wileyonlinelibrary.com.]

The quantity of heat absorbed during the melting of the polymer was substantively equivalent to that required to break down the crystal structure. The higher the crystallinity (χ_c) was, the higher the melting heat was. χ_c was calculated with the following formula:

$$\chi_c = \left(\frac{\Delta H_m}{\Delta H_o}\right) \times 100\%$$

where ΔH_m is the melting enthalpy and ΔH_0 is the balanced melting enthalpy (the melting enthalpy of 100% crystallographic PA6 was 230 J/g).[27]

Spectroscopy Analysis. FTIR spectroscopy (NEXUS 570, Thermo Nicolet Nexus) was used to compare the variation in carbonyl and hydroxyl functional groups resulting from thermooxidative degradation. During the testing process, the samples quality had a constant value, and the quality proportion of the samples to KBr was fixed. The degree of degradation could be detected and quantified by the detection of the changes in the dipole moment related to the stretching–vibration of the functional groups.

SEM. SEM, observed on KYKY-2800B and SHU-SU1510 instruments (KYKY Technology Development Co., Ltd., China), was used to investigate the surfaces of the unaged and aged PA6/LGF samples. SEM graphs of the samples were recorded after the surfaces were gold-coated with an accelerating voltage of 25 kV.

RESULTS AND DISCUSSION

Mechanical Behavior

The mechanical properties of the PA6/LGF samples with different thermooxidative exposure times were investigated. The key mechanical properties (i.e., tensile strength, flexural strength, and notched impact strength) with thermooxidative aging are shown in Figure 2. The stabilized samples showed the same behavior as the unstabilized samples (see Figure 2). However, the unaged samples exhibited a higher tensile, flexural, and notched impact strength than the aged samples. However, the mechanical properties of the samples after 50 days of thermooxidative exposure were much higher than those of the pure ones. The mechanical strength of the samples aged for 50 days decreased moderately because of the combined effects of heat and oxygen. The tensile strength of the stabilized samples decreased 16.1%, the flexural strength decreased 18.8%, and the notched impact strength decreased 28.8% after 50 days of aging. The tensile strength of the pure samples decreased 23.2%, the flexural strength decreased 23.4%, and the notched impact strength decreased 30.9% after 50 days of aging. Better aging resistance was observed for the stabilized PA6/LGF samples with the addition of antioxidant. Obviously, the synergism of copper salt antioxidant with phosphorous acid antioxidant 168 contributed to the increase in the oxidative stability. On one hand, the copper atoms (Cu^{n+}) could form a kind of complex with the PA6 resin to protect the weak bonds of the PA6 macromolecular chain, which were the carbon–hydrogen bonds of the

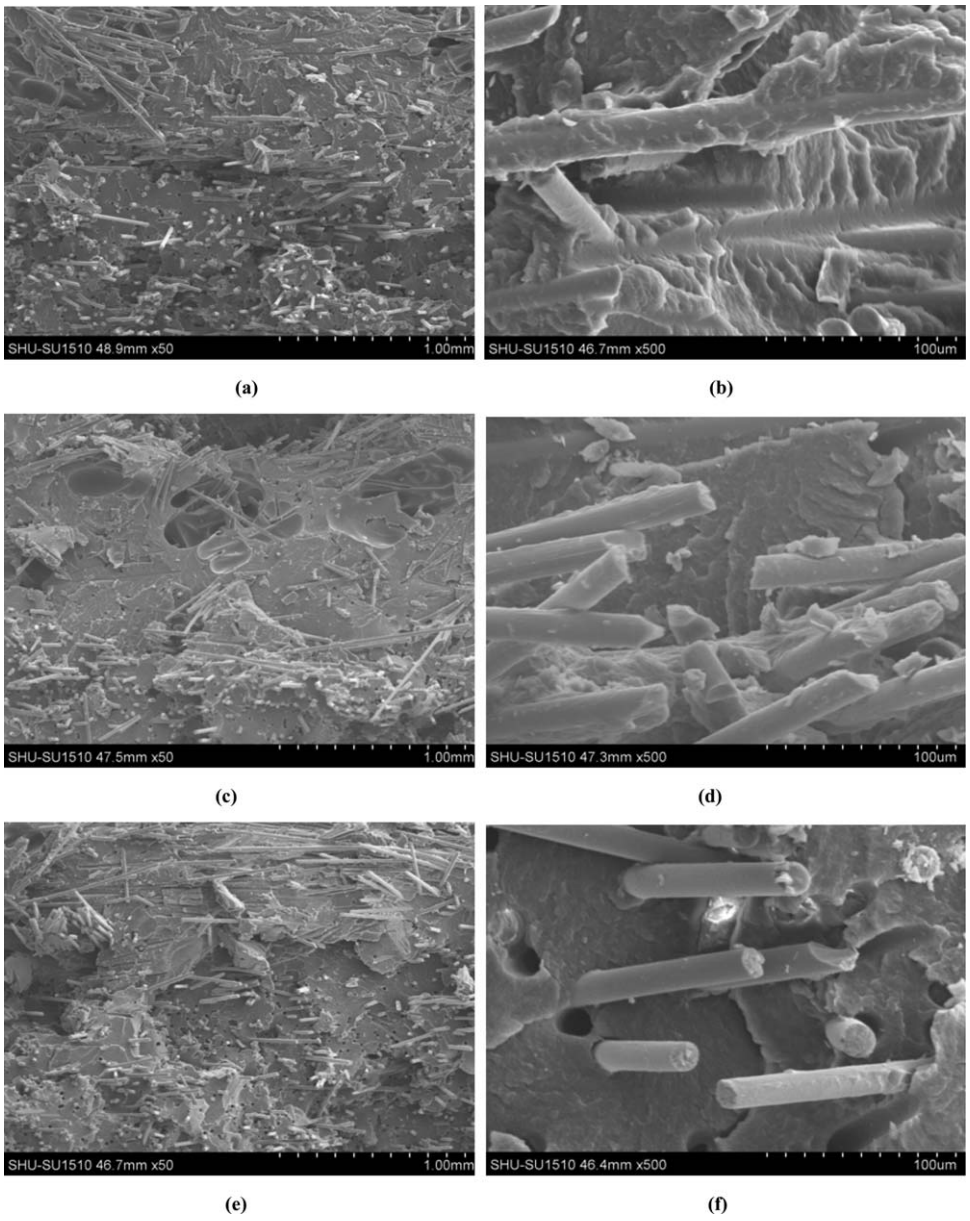

Figure 4. Scanning electronic micrographs of the tensile fractured surfaces of the (a,b) unaged PA6/LGF sample, (c,d) stabilized PA6/LGF sample, and (e,f) pure PA6/LGF sample after thermooxidative aging for 50 days.

methylenes adjacent to the carbonyl groups and nitrogen atoms. On the other hand, they could catalyze the existent hydroperoxides to decompose into nonradical products, which could prevent the formation of OH· radicals according to the following mechanism:[28]

$$\mathrm{ROOH} + \mathrm{M}^{n+} \rightarrow \mathrm{RO}\cdot + \mathrm{M}^{(n+1)+} + \mathrm{OH}^{-}$$

$$\mathrm{ROOH} + \mathrm{M}^{(n+1)+} \rightarrow \mathrm{ROO}\cdot + \mathrm{M}^{n+} + \mathrm{H}^{+}$$

The copper salt antioxidant synchronized with the phosphorous acid antioxidant 168 was beneficial for antithermal oxidative aging in the PA6/LGF composites because of its low consumption.

All of the mechanical properties of the aged PA6/LGF samples in the absence or presence of the stabilizers were analogous at 160°C. When the aging temperature was in the range of between the glass-transition temperature (T_g) to melting temperature (T_m) of resin, there was an annealing process of PA6 at first. In this case, the internal stress of PA6 decreased, whereas the spherulites of PA6 grew bigger and its χ_c increased.[21] As a result, we concluded that the notched impact strength and the brittleness of PA6/LGF decreased and rose, respectively. When the PA6/LGF samples were subjected to flexural stress, their degradation methods transformed from yield deformation to brittle fracture with the increase of aging time, which was classified as environment fracture.[15] However, the annealing process evolved into thermooxidative aging as the thermooxidative exposure time was prolonged, so the mechanical properties transformed from increasing to decreasing and showed a marked decrease as a function of the aging time in this study.

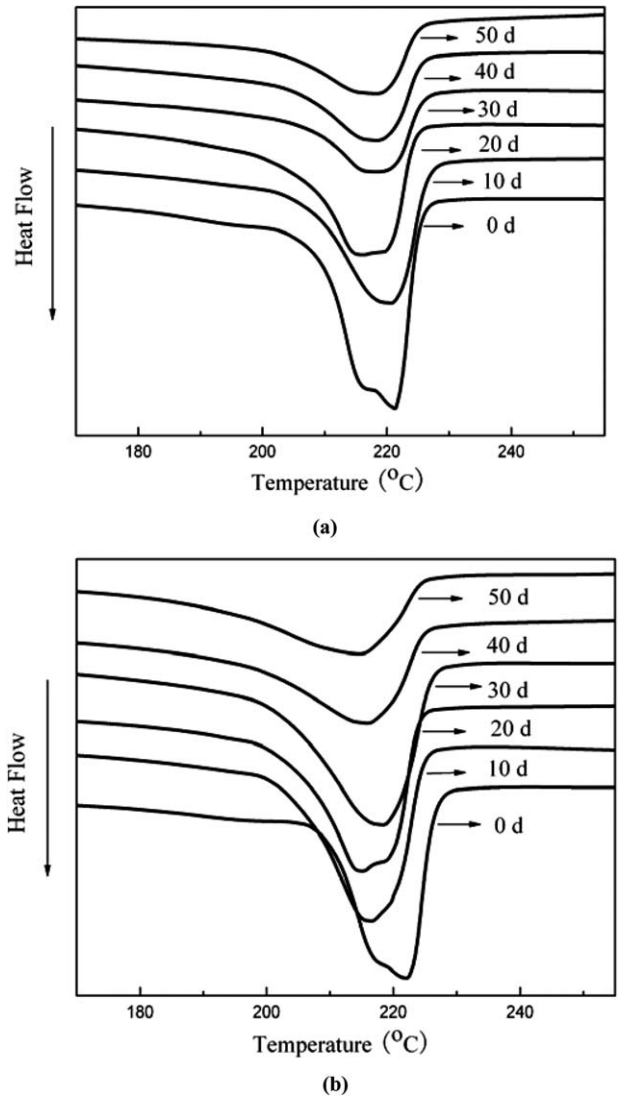

Figure 5. Melting curves of the DSC spectra for the thermally aged PA6/LGF samples: (a) pure LGF/PA6 and (b) stabilized LGF/PA6 as a function of the aging time.

Also, this phenomenon could be attributed to the decreases in χ_c and interfacial decohesion between the glass fibers and PA6 resin, which could be investigated by the latter means. Furthermore, significant intermolecular forces, which resulted from the formation of large numbers of van der Waal's interchain bonds and hydrogen bonding, become weak during the whole oxidation process.[19] Also, numerous defects appeared in the matrix

Table I. DSC Results for the Thermally Exposed and Stabilized PA6/LGF Samples

Exposure time (h)	0	10	20	30	40	50
T_m (°C)	222.2	218.3	216.6	215.0	215.9	214.6
T_c (°C)	189.6	189.3	189.9	188.5	188.0	186.5
χ_c (%)	34.8	32.2	30.5	28.7	28.2	24.4

Table II. DSC Results for the Thermally Exposed Pure PA6/LGF Samples

Exposure time (h)	0	10	20	30	40	50
T_m (°C)	221.3	218.3	218.3	218.2	216.8	216.0
T_c (°C)	190.8	190.6	189.2	189.1	189.3	186.9
χ_c (%)	36.2	28.7	26.0	24.8	22.5	21.4

or on the surface. Under the joint action of heat and oxygen, the polymer easily displayed automatic embrittlement of the oxidation reaction.[29] In particular, the combination of fibers and matrix properties and the ability to transfer stresses across the fiber–matrix interface influenced the mechanical performances of these glass-fiber-reinforced composites.[23] All of the aforementioned reasons resulted in the decline of the mechanical properties.

Microscopy Investigation

The SEM images of PA6/LGF after 0 and 50 days of aging are shown in Figure 3. The surface of the aged PA6/LGF was more rough than that of unaged one, and many sharp microcracks and surface damage were clearly observed in the whole region [Figure 3(b)]; these perhaps were produced by PA6 molecular chain decomposition. Some microcracks were parallel to the dispersed glass fibers; this led directly to interfacial debonding between the glass fibers and the PA6 matrix. Some grew with the dispersed glass fibers perpendicularly. The others grew like dispersive branches around the glass fibers, whereas there were almost no microcracks observed in the unaged PA6/LGF sample [Figure 3(a)]. Only a few blurry white strips on the surface represented the distribution of glass fibers in the PA6 matrix. On one hand, the aforementioned microcracks acted as Griffin flaws and crack initiation sites;[30] then, on the other hand, the increased amount of microcracks corresponded to the decreased fiber/matrix interface area, which could not provide higher pull-out forces. When the composites under the action of loading, the microcracks accelerated, growing into cracks and then

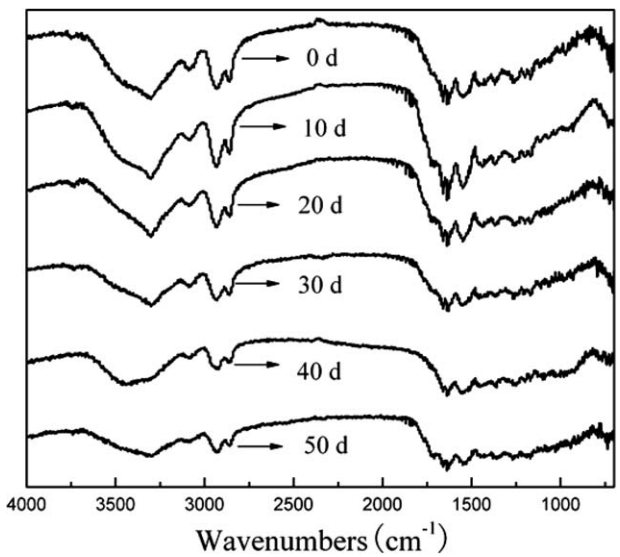

Figure 6. FTIR spectra of the thermally aged PA6/LGF samples.

Figure 7. Digital photos of the PA6/LGF samples as a function of the aging time at 160°C. [Color figure can be viewed in the online issue, which is available at wileyonlinelibrary.com.]

playing a major role in reducing the static mechanical properties. Moreover, much powder on the aged samples fell off; a possible reason was that the low-molecular-weight polymers and small molecules produced by the oxidation reaction were apt to form imperfect spherulites, which promoted thermal embrittlement.[29]

To further investigate the interfacial adhesion of the pure and stabilized PA6/LGF samples, in Figure 4(a,b), we show the typical SEM images of the tensile fractured surfaces of the unaged PA6/LGF composites, from which it can be clearly seen that the fracture mostly occurred in the matrix phase rather than in the interface between the glass fibers and resin. The fracture sections also show residual PA6 matrix adhere on the glass fibers surfaces of the unaged sample. Thus, it was implied that a high level of adhesion between the resin and the fiber was achieved. As is known, the fiber-reinforced composites absorbed tension energy via three major mechanisms: fiber breakage, fiber pullout, and matrix crack propagation.[6] The mechanical performances of these glass-fiber-reinforced composites resulted from a combination of the fibers and matrix properties and the ability to transfer stresses across the fiber–matrix interface. As the stress started to be applied on the composites, shear stresses were generated at the interfacial region to transfer the load from the matrix to the fibers.[8] Favored intermolecular interactions in the presence of PA6 chains resulted in a tangle of the PA6 sheathing layer.[15] However, the aged PA6 chains easily disentangled and slid because of the lack of strong chemical bonds in the interfacial region. Consequently, the pullout of the fibers took place at these weak adhesion zones. Figure 4(c–f) show the typical SEM images of the tensile fractured surfaces of the stabilized and pure PA6/LGF composites after they were subjected to thermooxidative aging for 50 days, although this kind of perfect fiber/matrix adhesion, shown in Figure 4(a,b), was not clearly evident in Figure 4(c–f), especially in Figure 4(e,f). Upon fracture of the stabilized PA6/LGF sample after 50 days of aging [Figure 4(c,d)], a few PA6 sheathing layers remained on the fiber surfaces; this indicated that the interfacial failure did not completely take place at these zones. As shown in Figure 4(e,f), many holes formed by the evulsion of glass fibers were found remaining in the tensile fractured surface of the pure PA6/LGF samples, and this number was also greater than that of the stabilized one after 50 days of aging; this indicated the comparatively poor adhesion of the glass fibers with the resin. Upon fracturing of the pure PA6/LGF samples, there was no PA6 sheathing layer remaining on the glass fiber surfaces; this indicated that interfacial failure took place at these zones. Also, the fibers were debonded, leaving a dark ring at the interface. In the study of Fu and Lauke,[31] the dark rings resulted from local deformation of the matrix around the fibers after fiber debonding. The previous results can possibly explain why the static mechanical properties of the unaged PA6/LGF samples showed a better mechanical performance than the aged ones; also, we came to the same conclusion for the results between the stabilized and pure PA6/LGF samples. Actually, the antioxidants significantly retarded the rate of PA6 degradation by interfering with radical propagation; as a result, the stabilized PA6/LGF samples reserved a more basic structure and groups than the pure ones. To some extent, strong chemical bonding may have remained on the interface of the glass fibers and PA6 chains or the separate molecular chains, and the probability of depolymerization and chain sliding at the interface of the stabilized samples was much lower than that of the pure ones. Consequently, these weakly entangled zones were replaced by the pulled-out fibers. Therefore, the pure PA6/LGF samples exhibited poor interfacial interaction, which led to markedly reduced mechanical properties during thermooxidative aging.

Crystallization Behavior

The DSC thermographs of the unaged and aged PA6/LGF samples are shown in Figure 5. χ_c was calculated by integration of the area under the DSC melting endothermic peak and division by the heat of fusion with 100% crystalline PA6 ($\Delta H_0 \approx 230$ J/g).[32] Tables I and II give the summary of the DSC tests results. The increase in the thermooxidative exposure time of the pure and stabilized PA6/LGF samples had a quite strong effect on T_m, crystallization temperature (T_c), and χ_c. When the stabilized samples were aged for 50 days, decreases of 8°C in T_m and 3°C in T_c and a significant decrease (~10%) in χ_c were observed. The pure samples showed decreases of 5°C in T_m and 4°C in T_c and a significant decrease (~15%) in χ_c. The decreases appeared to be strongly responsible for the weakening of the mechanical properties in the aged PA6/LGF samples, especially for the pure samples. During the thermooxidative aging process, a

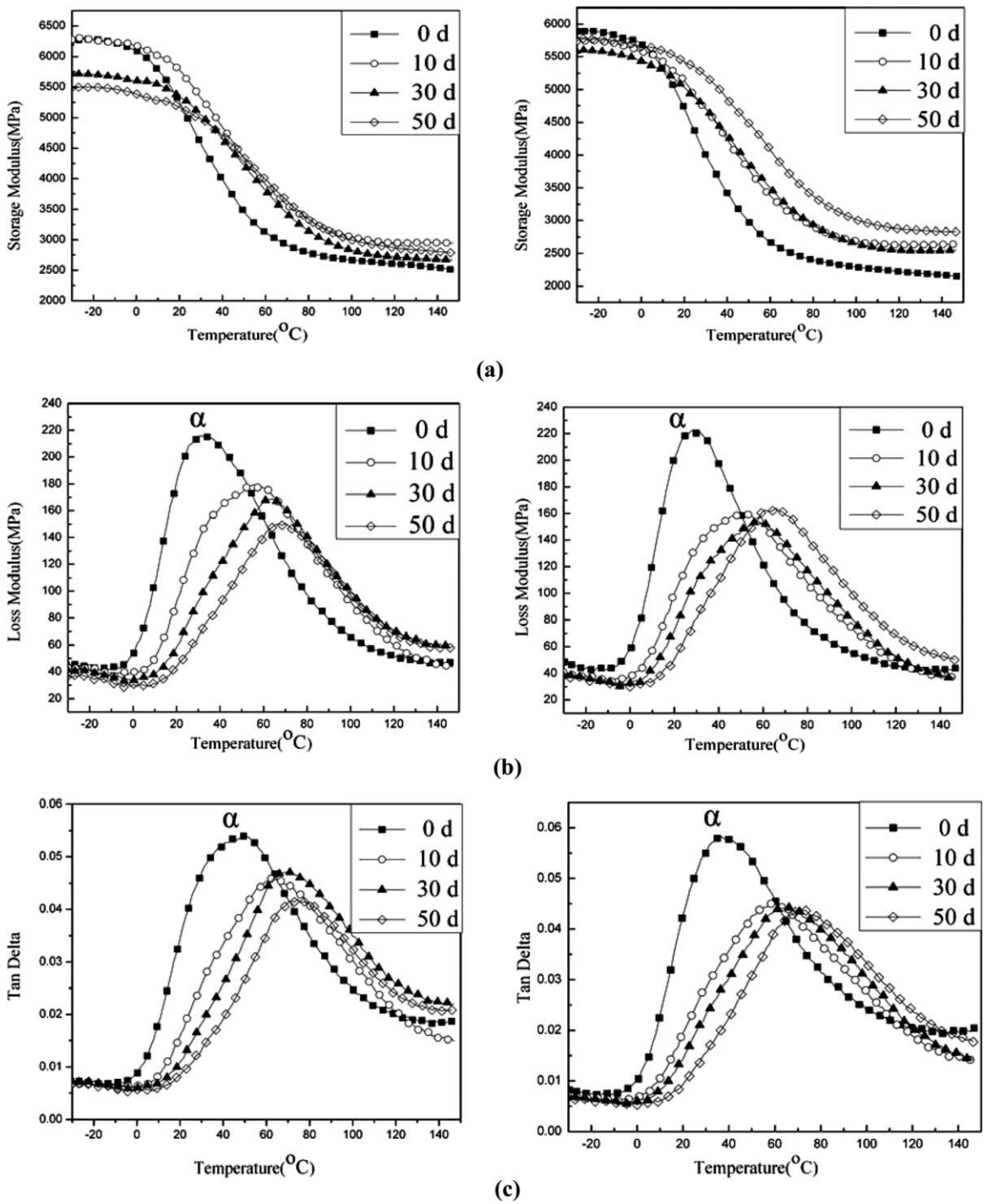

Figure 8. DMA spectra of the PA6/LGF samples as a function of the aging time at 160°C: (a) storage modulus of the pure and stabilized PA6/LGF samples, (b) loss modulus of the pure and stabilized PA6/LGF samples, and (c) tan δ of the pure and stabilized PA6/LGF samples.

concentration of weakness rose in amorphous region, which accelerated the oxidation degradation in the noncrystalline region without a doubt.[19]

FTIR Analysis

FTIR analysis was conducted to evaluate the degree of degradation.[9] Polyamides commonly have a —CONH— bond. Figure 6 shows the IR spectrum of the unaged and aged PA6/LGF samples; the representative amide peaks I and II were found at 1640 and 1540 cm^{-1}. Furthermore, the absorption peaks at 3300, 3070, 2960, and 2860 cm^{-1} represented —NH, —CH_2, and —CH, respectively. The absorption bands arising around 1710 and 1760 cm^{-1} corresponded to carbonyls originating from the carboxyl functional groups (e.g., ketones at 1715 cm^{-1}, aldehydes at 1725 cm^{-1}, aliphatic carboxylic acids at 1750 cm^{-1}, and esters at 1735 cm^{-1}),[21] which were insensitive

Table III. T_g and Tan δ_{max} Values for the Stabilized PA6/LGF Samples as a Function of the Aging Time at 160°C

Exposure time (days)	0	10	30	50
T_g (°C)	28.06	49.89	57.73	65.89
Tan δ_{max}	0.05814	0.04505	0.04422	0.04366

to oxidation. Dong and Gijsman[22] inferred that the chromophore structure was α-keto carboxyl, and the yellow substance might have been $NH_2CH_2CH_2CH_2CH_2COCOOH$ or $NH_2CH_2CH_2CH_2COCOOCH_3$ or their mixture because both molecules have a molecular weight of 145 (α-keto carboxyl and amino groups). As shown in Figure 7, the surface color of the pure samples was darker than that of the stabilized ones during the first 30 days. It was obvious that the antioxidant additives effectively inhibited the yellowing of the PA6/LGF samples. The broad peak indicated that —NH, —CH_2, —CH, and amide peaks were also weakened by thermooxidative treatment. Decreases in the intensities of these polyamide representative bands were observed as the aging time increased. This result suggested that the representative polyamide groups (N—H and C—H) locally underwent oxidation on the PA6/LGF sample surface because of thermal degradation.

Dynamic Mechanical Behavior of the PA6/LGF Composites

The main objective of this experiment was to apply DMA to the aging study of the pure and stabilized PA6/LGF samples. In Figure 8, the storage modulus, loss factor, and damping factor (tan δ) values for the unaged and aged samples of the pure and stabilized PA6/LGF samples are shown as a function of the temperature at a frequency of 10 Hz. As shown in Figure 8(a), the magnitude of the storage modulus of the pure and stabilized PA6/LGF samples decreased linearly as a function of the temperature in the glassy region, and its values in the aged samples were higher than in the unaged ones. As shown in Figure 8(b,c), there was only one transition peak for the loss modulus and tan δ curve; this corresponded to α relaxation arising from the chain segmental motion of the molecules. At this point, it was necessary to make certain considerations. Furthermore, the segregation of soft segment and the expected formation of domain structures for PA6 had to be taken into account. The α relaxation temperature is usually defined as T_g of the polymers. For the pure and stabilized PA6/LGF samples aged for 0, 10, 30, and 50 days, the tan δ curves shifted to higher temperatures compared with the samples that were not aged. This resulted in an increase in T_g, which was caused by the resin molecular chain crosslinking reaction during the primary aging stage.

Table IV. T_g and Tan δ_{max} Values for the Pure PA6/LGF Samples as a Function of the Aging Time at 160°C

Exposure time (days)	0	10	30	50
T_g (°C)	30.72	55.66	64.37	70.09
Tan δ_{max}	0.05393	0.04586	0.04713	0.04190

However, the molecular degradation predominated during the later stage of aging, and the amorphous region expanded.[19] The corresponding parameters of DMA are listed in Tables III and IV.

All restrictions on the mobility of the main chain of PA6 were expected to decrease the peak area of the loss modulus, which would also be reflected in the tan δ peak intensity. Therefore, the tan δ peak intensity at the relaxation temperature (tan δ_{max}) was considered to reflect the extent of the mobility of the macromolecular chain segments.[33] Both the peak area of the loss modulus and the peak intensity of tan δ_{max} of the aged samples were lower than those of the unaged samples, and the results were the same between the pure and stabilized samples. This implied that the mobility of the molecules and the damping properties of PA6 were reduced during thermooxidative aging. In the composite materials, there were numerous decreased damping cases, such as the reduced damping in the PA6 matrix near the interface because of the increased thermal stresses or changes in the polymer conformation or morphology.[20] At temperatures below T_g, the damping could be small. The widespread transition around T_g could possibly have been due to short hard-segment units and could have also been related to an interface of the polymer weakly adsorbed on the surfaces of the filler, such as the glass fibers. Obviously, even though both thermal embrittlement and oxidative embrittlement would make the chain relaxation much difficult because of the crosslinking of molecules, the aggregation of weakness arose in the amorphous region; however, molecular chain crosslinking predominated during the aging process.

CONCLUSIONS

The effects of thermooxidative aging on the static and dynamic mechanical properties of both the pure and stabilized PA6/LGF composites were examined at a temperature of 160°C. The experimental findings indicated that the interfacial debonding between the PA6 resin and glass fibers, the decreased χ_c, and the variation in the molecular chain structure in the PA6/LGF composites appeared to be responsible for the variations in static and dynamic mechanical properties. The influence of the thermooxidative aging on the PA6/LGF composites was also investigated with DSC, SEM, FTIR spectroscopy, and DMA measurements. The decreases in the static mechanical properties, χ_c, and interfacial cohesion and the increases in the T_g, amorphous region crosslinking, and carboxyl functional groups were definably observed as thermooxidative aging proceeded. SEM observations indicated that the tensile fractured surfaces of the thermally aged pure and stabilized PA6/LGF composites showed a phenomenon of pulled-out fibers, and fracture mostly occurred in the interface between the glass fibers and the matrix rather than in the matrix phase. Many sharp microcracks and powder were clearly observed on the whole aged surface region; this indicated that the PA6/LGF composites were obviously degraded by thermooxidative aging. The DMA measurement appeared to be an effective method for quantifying the influence of aging on the PA6/LGF composites. Thermooxidative aging occurred primarily in the amorphous region of the polymer; the rise in T_g and the reduction of the mobility of PA6 molecules

after aging were caused by the molecular chain crosslinking reaction. The stabilizers endowed the PA6/LGF composites with better static and dynamic mechanical properties compared with the composites with no stabilizers. The longer the aging time was, the more remarkable the function of the stabilizers was.

ACKNOWLEDGMENTS

The authors are grateful for the financial support provided for this research by Industrial Revitalization of Science Projects [contract grant number 2012101(1–7)] and the Innovation Fund of Guizhou University (contract grant number 2013067).

REFERENCES

1. Truckenmuller, F.; Fritz, H. G. *Polym. Eng. Sci.* **1991**, *31*, 1316.
2. Takeshi, M. *Compos. A* **1996**, *27*, 379.
3. Yan, W.; Han, K.; Qin, L.; Yu, M. *J. Appl. Polym. Sci.* **2004**, *91*, 3959.
4. Huang, X. H.; Li, B.; Shi, B. L.; Li, L. P. *Polymer* **2008**, *49*, 1049.
5. Carlsoon, L. A.; Pipes, R. B. Thermoplastic Composite Materials; Elsevier: New York, **1991**; p 171.
6. Han, K.; Liu, Z.; Yu, M. *Macromol. Mater. Eng.* **2005**, *290*, 688.
7. Vauthier, E.; Chateauminois, A.; Bailliez, T. In Proceedings of the Tenth International Conference on Composite Materials; Poursartip, A., Street. K., Eds.; Woodhead Publishing: Cambridge, UK, **1995**; Vol. *6*, p 185.
8. Kennedy, M. T.; Cuellar, E.; Roberts, D. R. Proc. Soc. Photo-Opt. Instrum. Eng. **1992**, *1791*, 67.
9. Liao, K. *J. Mater. Sci. Lett.* **1999**, *18*, 763.
10. Thomason, J. L. *Polym. Compos.* **2006**, *27*, 552.
11. Thomason, J. L. *Polym. Compos.* **2007**, *27*, 331.
12. Thomason, J. L. *Polym. Compos.* **2007**, *27*, 344.
13. Lánská, B.; Makarov, G. G.; Sebenda, J. *Angew. Makromol. Chem.* **1990**, *181*, 143.
14. Lánská, B. *Eur. Polym.* **1994**, *30*, 197.
15. Matisova-Rychla, L.; Lanska, B.; Rychly, J. *Angew. Makromol. Chem.* **1994**, *216*, 169.
16. Koen, J.; Pieter, G.; Daan, T. *Polym. Degrad. Stab.* **1995**, *49*, 127.
17. Pieter, G.; Daan, T.; Koen, J. *Polym. Degrad. Stab.* **1995**, *49*, 121.
18. Pieter, G.; Mike, K.; Mieke, O. *Polym. Degrad. Stab.* **1996**, *51*, 3.
19. Shu, Y.; Ye, L.; Yang, T. *J. Appl. Polym. Sci.* **2008**, *110*, 945.
20. Dan, F.; Bjorn, T. *Polym. Degrad. Stab.* **2000**, *67*, 69.
21. Šebenda, J.; Lánská, B. *J. Macromol. Sci. Pure Appl. Chem.* **1993**, *30*, 669.
22. Dong, W.; Pieter, G. *Polym. Degrad. Stab.* **2010**, *95*, 1054.
23. Zinck, P.; Gerard, J. F. *Polymer* **2001**, *42*, 6641.
24. Li, Z. H.; Chen, S. J.; Zhang, J. *Plast. Rubber Compos.* **2009**, *38*,187.
25. Lotkova, H.; Kucera, O. *Physiol. Res.* **2009**, *58*, 685.
26. Janssen, K.; Gijsman, P.; Tummers, D. *Polym. Degrad. Stab.* **1995**, *4*, 127.
27. Dan, F.; Bjorn, T. *Polym. Degrad. Stab.* **2000**, *67*, 69.
28. Bauer, I. *Polym. Degrad. Stab.* **1995**, *48*, 427.
29. Sanshuo, W. The Aging of Plastic; Defense Industry Press: Beijing, **1977**.
30. Al-Malaika, S. Atmospheric Oxidation and Antioxidants; Elsevier: Amsterdam, **1993**; p 45.
31. Fu, Y. S.; Lauke, B. *Compos. Sci. Technol.* **1997**, *32*, 1985.
32. Jong-Il, W. *Polym. Degrad. Stab.* **2010**, *95*, 14.
33. Perera, M. C. S.; Ishiaku, U. S.; Ishak, Z. A. M. *Polym. Degrad. Stab.* **2000**, *68*, 393.